

Supplementary Methods

1.i Illustrative plot of heart rate parsing

Supplementary Results

2.i Heart rate parsing - separation into high and low frequency variability

2.ii Topoplots in 100ms bins

2.iii Relationship of high and low frequency variability to ERP responses.

2.iv Description of Ex-Gaussian Response Distribution fitting

2.v Analysis examining within-participant changes in heart rate

Supplementary Methods

1.i Illustrative plot of heart rate parsing

Figure S1 shows an illustrative plot of the data visualisations used to perform manual setting of the thresholds for ECG data parsing, and for post hoc checking of the accuracy of the results.

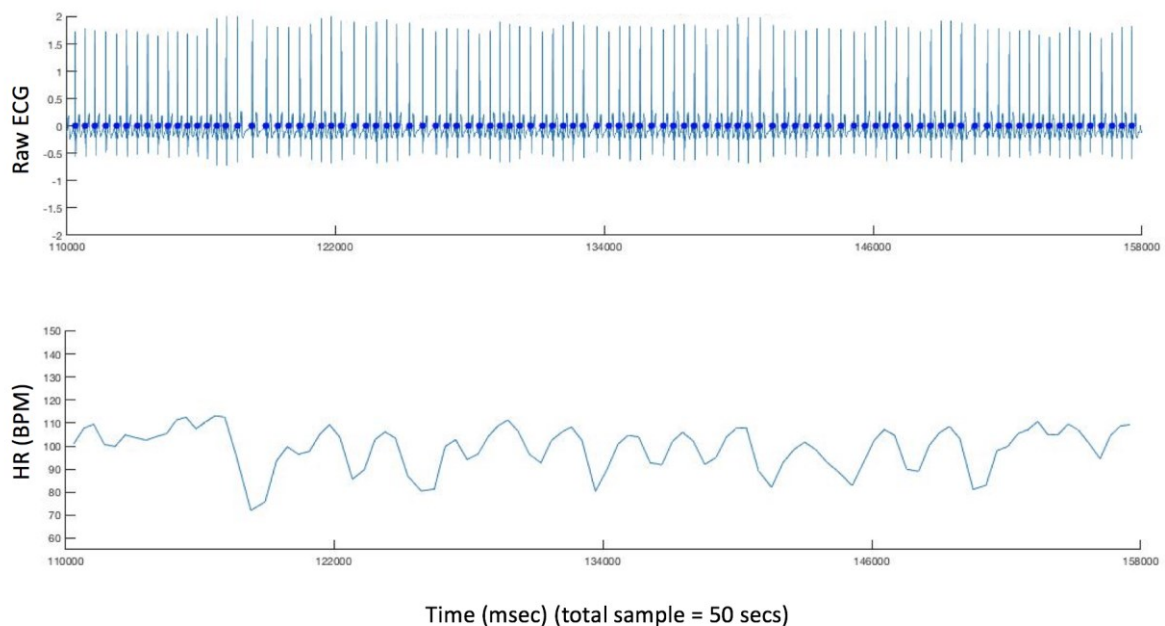


Figure S1: Demonstration of HR parsing of raw ECG data. Raw ECG data were recorded (top) and parsed using a variable amplitude threshold. The amplitude threshold was inspected and adjusted between participants based on the data visualisation shown, which allowed for falsely identified beats to be easily identified via visual inspection. The blue dots indicate the heart beats identified by the computer algorithm. Any falsely identified beats were identified using the automatic artefact rejection criteria described in the main text. The bottom plot shows the HR (in Beats Per Minute) derived from the individual beats shown in the plot above. As a final check, visual inspection of the data was conducted by examining both of these plots in order to identify any falsely identified heart beats.

Supplementary Results

2.i Heart rate parsing - separation into high and low frequency variability

Figure S2 shows the raw HR data collected during the experiment, rank ordered by mean HR obtained across the entire trial. This figure illustrates two clear parameters of variability in our data: first, they show consistent between-participant differences in mean HR, which is the focus of the analyses featured in the main text. Second, they show between-participant differences in heart rate variability. The analyses presented here examine this.

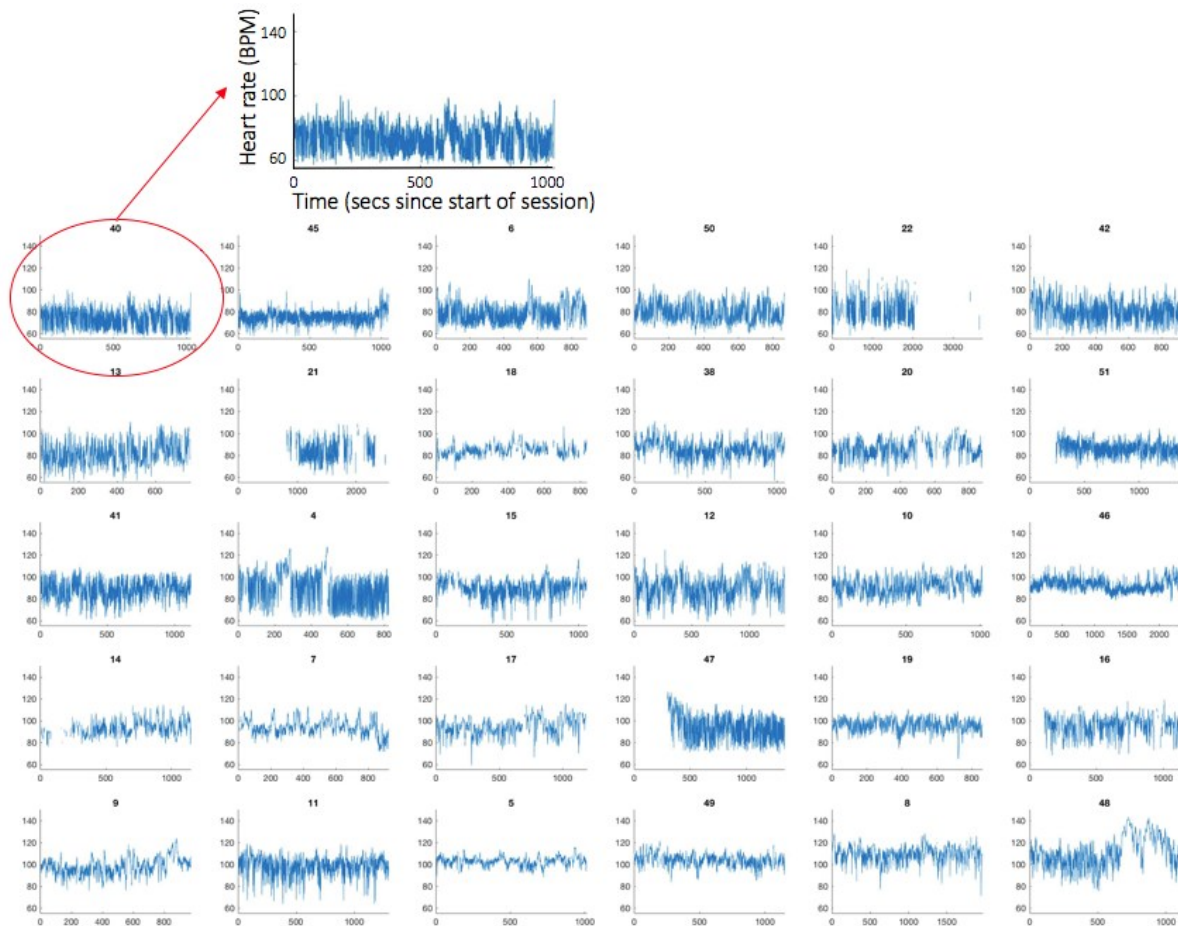
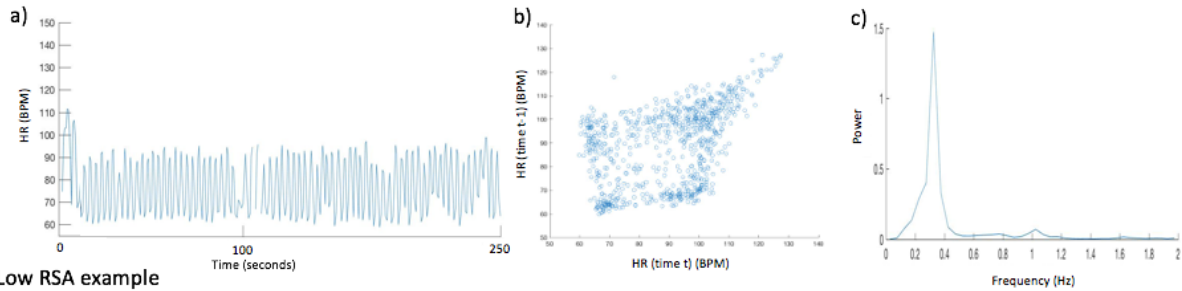


Figure S2: Raw heart rate data for all participants included, sorted by mean heart rate from top left (lowest mean HR) to bottom right (highest). A number of features of the heart rate data can be seen in these images: high-frequency fluctuations (vagal mediated changes, known as RSA) as well as low frequency fluctuations. These differences are examined further in the Supplementary Materials.

High RSA example



Low RSA example

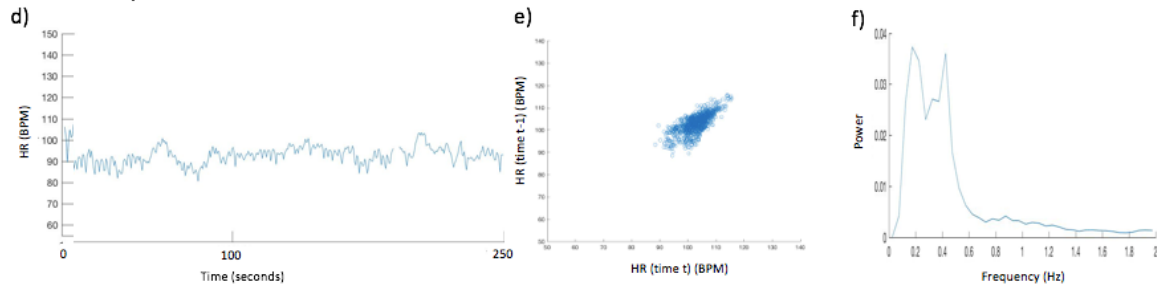


Figure S3: Illustration of two datasets from participants showing high and low Respiratory Sinus Arrhythmia (RSA). Plots a), b) and c) show data from a participant showing high RSA. a) raw time series of HR fluctuations over time (4 minute data sample); b) Poincaré plot showing HR at time t on x-axis and HR at time $t+1$ (the heart beat immediately following) on y-axis; c) Fourier plot showing a peak frequency at c.0.35Hz (corresponding to the respiration cycle). Plots d), e) and f) show identical plots from another participant showing low RSA. d) raw time series of HR fluctuations over time; e) Poincaré plot; f) Fourier plot showing a no clear peak in activity with the respiration cycle.

High-frequency variability. In order to quantify these differences we conducted analyses to examine HR variability in both the frequency and time domains, following the standard procedures (Porges, 1995). First, in order to estimate variability in the time domain, the variability between consecutive valid heart beats was estimated by calculating the Root Mean Square of Successive Differences (RMSSD). Second, in order to estimate variability in the frequency domain, the continuous heart beat data were epoched into evenly spaced 250 ms bins, linear interpolation was performed to cover short periods of missing data, and a Fourier transform was calculated. Based on previous research (Bush, Alkon, Obradović, Stamperdahl, & Boyce, 2011) suggesting that the respiration period in children of this age tends to be with the 0.15-0.8Hz, high-frequency variability was calculated as the natural logarithm of the total power within this frequency range. Our analyses (see Supplementary Figure S7) suggested a strong association between the time domain and frequency domain approaches used to estimate high-frequency variability $\rho(29)=.83$, $p<.001$, and so only one measure, RMSSD, was used in subsequent analyses. Figure S4 shows the raw HR data rank ordered by RMSSD. As expected (based on e.g. Cacioppo, Tassinari, & Berntson, 2000) a strong negative association was observed between RMSSD and mean HR ($\rho(29)=-.76$, $p<.001$), such that more high-frequency variability was associated with lower mean HR (Figure S7d).

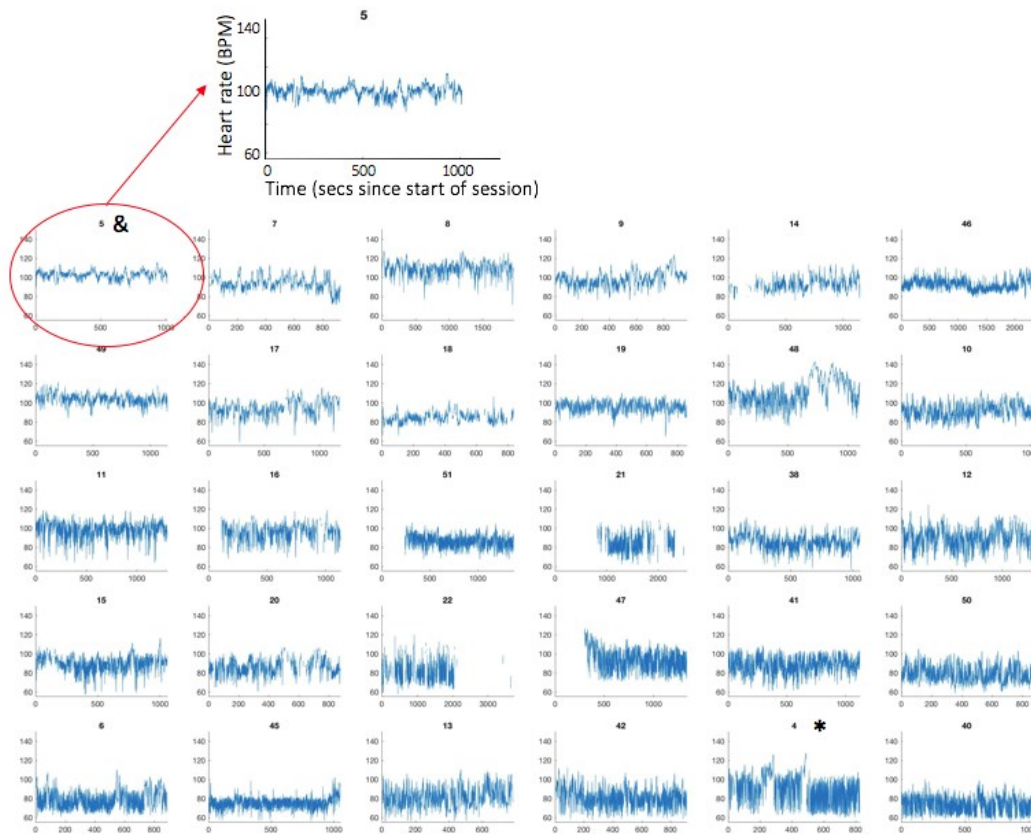
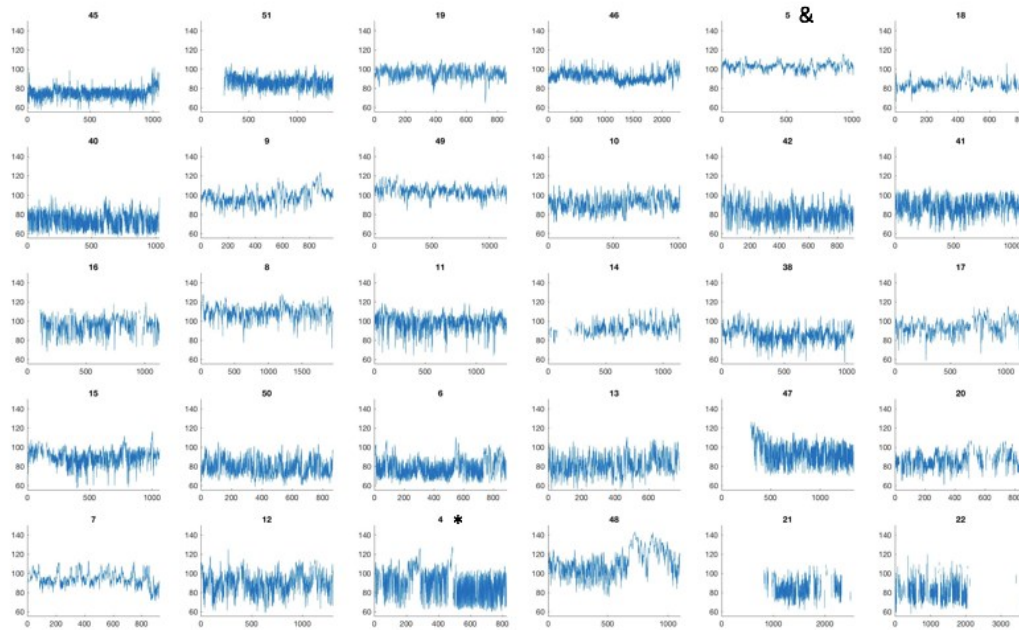


Figure S4: Raw HR data, rank ordered by RMSSD from lowest variability (top-left) to highest variability (bottom-right). The numbers above the plots show the participant number. The ‘high RSA’ sample illustrated in Figure S2 is highlighted with a * (bottom right on this plot). The ‘low RSA’ illustrated in Figure S2 is highlighted with a & (top left on this plot).

Low-frequency variability. In addition we wished to quantify low-frequency variability in our HR data, following from previous research that has suggested that low-frequency variability may have a dominant sympathetic contribution (e.g. Berntson et al., 1997; although see Billman, 2013; Reyes del Paso, Langewitz, Mulder, Roon, & Duschek, 2013). Again, we estimated low-frequency variability in both the time domain and the frequency domain. First, to estimate variability in the time domain, we down-sampled the data to 20-second time bins and recalculated the RMSSD (henceforth RMSSD_Low). Thus, rather than looking at variability between individual heart beats, this measure indexes variability in HR between individual 20-second epochs. Second, to estimate variability in the frequency domain, we summed the total activity in the $<0.15\text{Hz}$ range, based on the results of the Fourier analysis described above. Our analyses (see Supplementary Figure S7b) identified a strong association between the time domain and frequency domain approaches used to estimate low-frequency variability $\rho(29)=.81, p<.001$, and so only one measure, RMSSD_Low, was used in subsequent analyses. No relationship was observed between RMSSD_Low and mean HR $\rho(29)=-.08, p=.69$. Figure S5 shows the raw HR data rank ordered by RMSSD_Low.



*Figure S5: Raw HR data, rank ordered by RMSSD_{low} from lowest variability (top-left) to highest variability (bottom-right). The numbers above the plots show the participant number. As in Figure S4, the x axis shows the time (in seconds since the start of the session), and the y axis shows heart rate in beats per minute. The ‘high RSA’ sample illustrated in Figure S3 is highlighted with a * (bottom right on this plot). The ‘low RSA’ illustrated in Figure S3 is highlighted with a & (top left on this plot). Of note, and although low-frequency variability is often discussed in the literature as an index of sympathetic nervous system, the rank orderings of these datasets is quite similar between this plot and Figure S4. This point is discussed further in the Discussion in the main text.*

In addition we also calculated the HF/LF ratio, which is sometimes thought to index sympatho-vagal balance (Berntson et al., 1997; although see Billman, 2013; Porges, 2007). This was calculated by dividing the low- and the high-frequency variability. A strong negative relationship was observed between HF/LF ratio and mean HR $\rho(29)=-.68$, $p<.001$, suggesting that a higher ratio of HF to LF activity associates with lower HR.

2.ii Topoplots in 100ms bins

For the analyses presented in the main text we have presented topoplots only for the time windows corresponding to the main ERP peaks. Here (Figure S6), we additionally present topoplots in regularly spaced intervals between 100ms intervals from -100ms pre-stimulus to 500ms post-stimulus. 100ms intervals have been chosen for these plots because, consistent with previous research (Kushnerenko, Ceponiene, Balan, Fellman, & Näätänen, 2002), peaks were observed to be more long-lasting than comparable studies with adult populations.

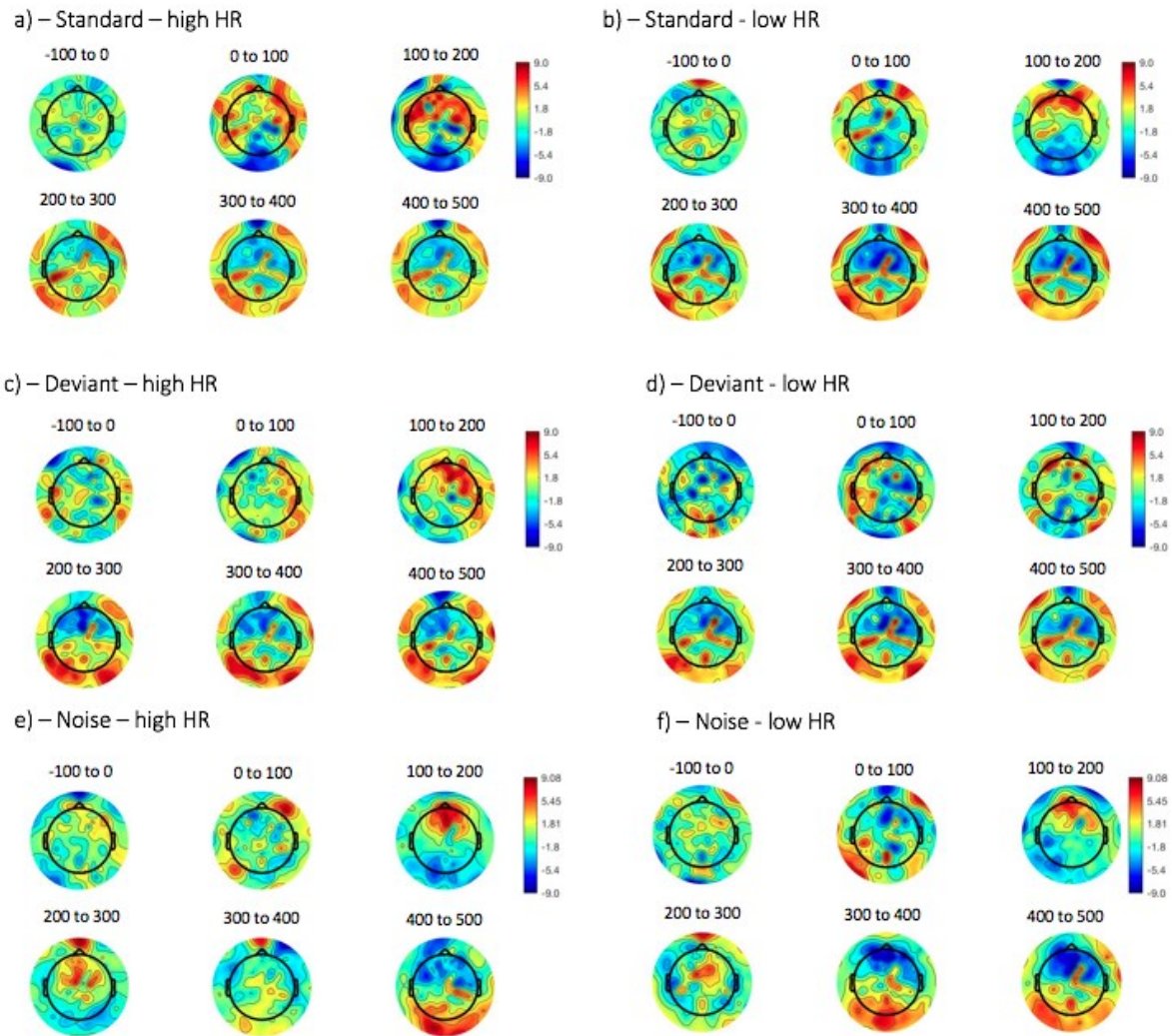


Figure S6: topoplots for responses to all trials, split by the participants' mean HR across the entire testing session and binned into 100 ms time intervals. The figure above each time plot indicates the mean time of each bin, in ms, relative to stimulus onset. The colour bar indicates the voltage, in μV . a) Standard - high HR group; b) Standard - low HR group; c) Deviant - high HR group; d) Deviant - low HR group; e) Noise - high HR group; f) Noise - low HR group.

2.iii Relationship of high and low frequency variability to ERP responses.

RMSSD showed a marginally non-significant relationship with N250 Standard amplitude $\rho(20)=-.43$, $p=.051$, such that higher variability was associated with larger ERP amplitudes (Figure S8a). Figure S9 shows the averaged ERP responses, subdivided by high/low RMSSD. The results are highly similar to those obtained when results are subdivided by high/low mean HR (Figures 2c, 4c, 5c).

RMSSD_{Low} showed a significant relationship with N250 Standard amplitude $\rho(20)=.44$, $p=.048$ (Figure S8b). HF/LF ratio showed a significant relationship with N250 Standard amplitude $\rho(20)=-.51$, $p=.02$, suggesting that an increased ratio of High- to Low-Frequency activity was associated with larger amplitude ERP responses.

Relationships of the variability measures to P150 Deviant responses were also consistent with those reported in the main text, with comparable but marginally smaller effect sizes (Figure S8d-f). Overall, the relationships observed between HR variability and the ERP responses were as predicted based on the relationships between mean HR and ERP responses shown in the main text, and between mean HR and HR variability shown in the Figure S7.

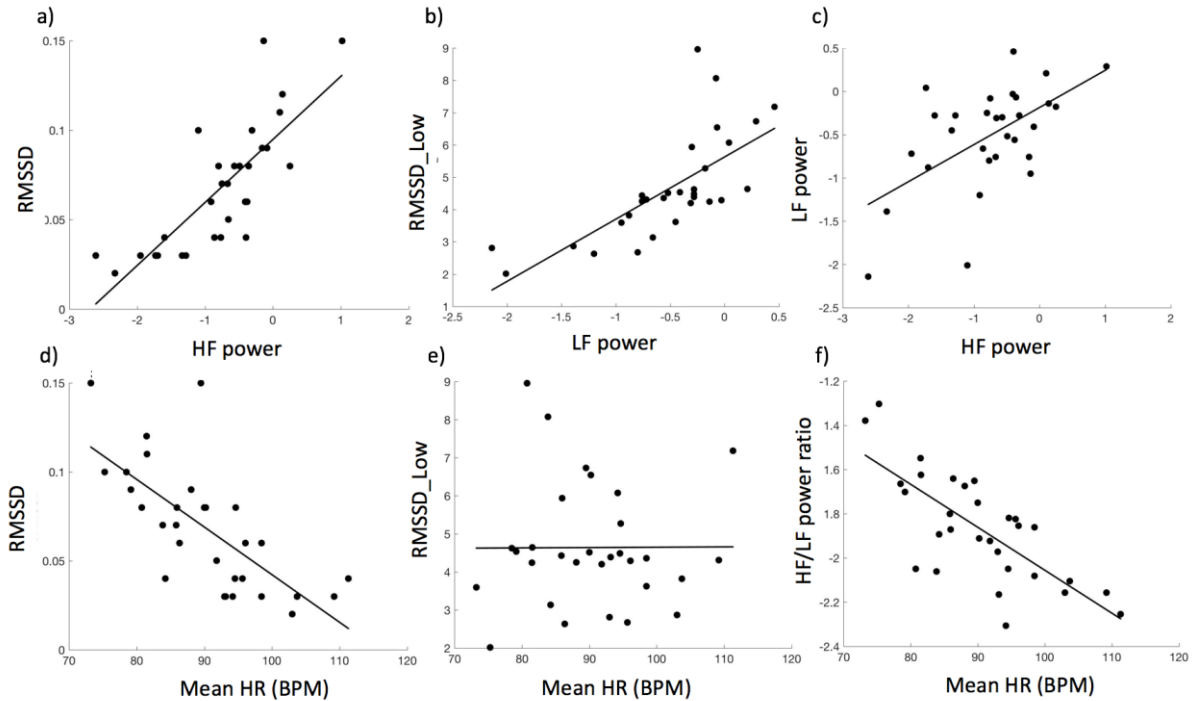


Figure S7: a) scatterplot showing the relationship between high-frequency power (total power 0.15-0.8 Hz) and RMSSD; b) scatterplot showing the relationship between low-frequency power (total power <0.15 Hz) and RMSSD_Low (variability between 20-second epochs); c) scatterplot showing the relationship between low- and high-frequency power; d) scatterplot showing the relationship between RMSSD and mean HR; e) scatterplot showing the relationship between RMSSD_Low and mean HR; f) scatterplot showing the relationship between HF/LF ratio and mean HR.

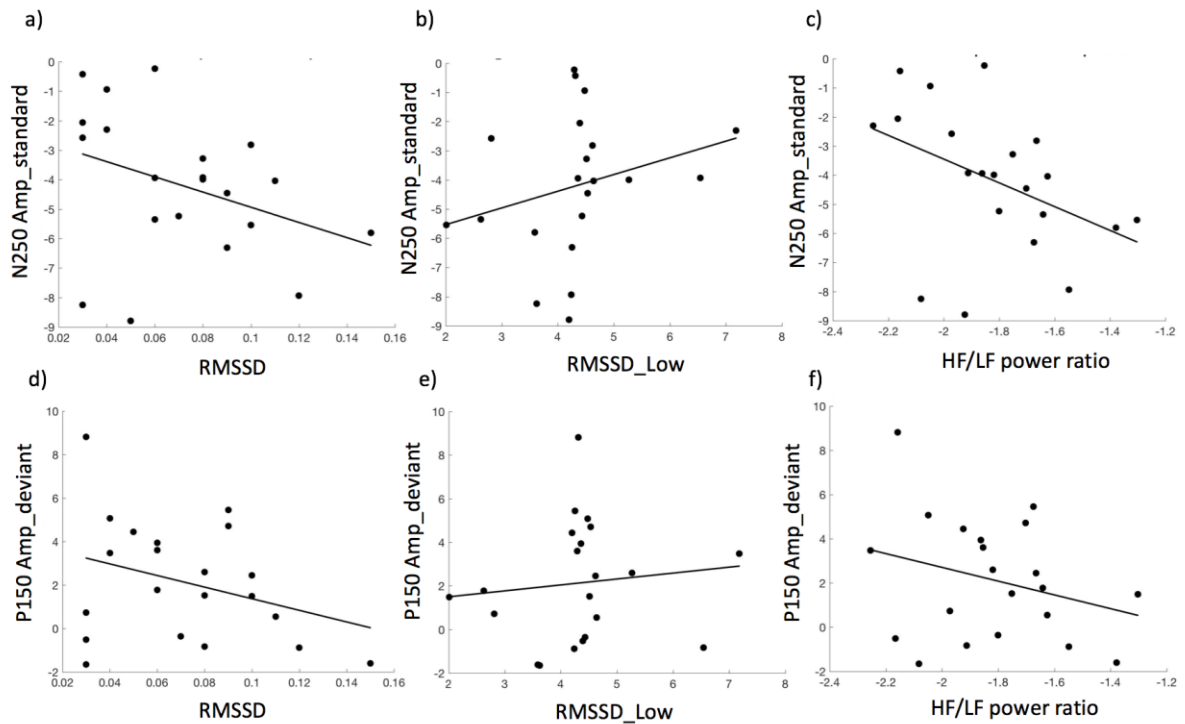


Figure S8: a) scatterplot showing the relationship between RMSSD and N250 Standard amplitude; b) scatterplot showing the relationship between RMSSD_Low and N250 Standard amplitude; c) scatterplot showing the relationship between HF/LF ratio and N250 Standard amplitude; d) scatterplot showing the relationship between RMSSD and P150 Deviant amplitude; e) scatterplot showing the relationship between RMSSD_Low and P150 Deviant amplitude; f) scatterplot showing the relationship between HF/LF ratio and P150 Deviant amplitude.

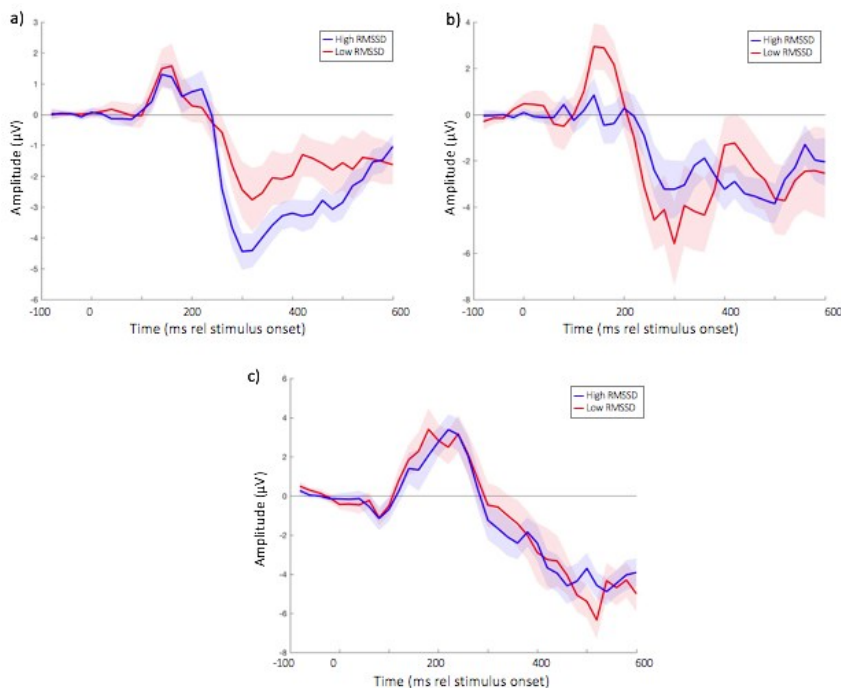


Figure S9: Averaged ERP responses, subdivided by participants using a median split by high/low RMSSD. a) Standard trials; b) Deviant trials; c) Noise trials. Shaded areas shown the error bars, calculated as Standard Error of the Mean.

2.iv Description of Ex-Gaussian Response Distribution fitting

A number of different distributions could have been used for this purpose, since the aim was not to find the best-fit but to compare parameters between distributions; the ex-Gaussian was selected as generally suitable given the shape of the data, although other distributions such as the gamma, lognormal or inverse Gaussian, could have been used instead (Johnson, Kotz, & Balakrishnan, 1994). The three components of the ex-Gaussian distribution describe, respectively, μ , the mode of the Gaussian component of the distribution; σ , the variance of the Gaussian component; and τ , the exponential (similar to the skewedness) (Lacouture & Cousineau, 2008).

For Standard Trials, results suggested that μ (mode of the Gaussian) was similar between the distributions: 87.3 for high HR and 88.5 for low HR. σ (variance of the Gaussian) was, however, markedly higher for the high HR group (14.8) than the low HR group (11.8). τ (exponential component) was also higher for the high HR group (0.43) than the low HR group (0.34). These results suggest that the modal responses are similar across the two populations, but that both components of response variability were larger in the high HR group.

For Deviant Trials, results suggested that μ (mode of the Gaussian) was again similar between the distributions – 98.4 for high HR and 99.1 for low HR. σ (variance of the Gaussian) was similar between the high and low HR groups: 7.6 for high HR and 8.1 for low HR. τ (exponential component) was markedly higher for the high HR group (10.9) than the low HR group (6.4). These results suggest that, whereas the modal responses were again similar between the two groups (shown by the similar μ components), the high HR group showed a sub-group of trials with a high response amplitude, manifesting as an increased τ (exponential component).

2.v Analysis examining within-participant changes in heart rate

The analyses presented in the main text examine between-participant differences based on mean HR recorded across the entire testing session. In addition, we wished to examine whether similar patterns could be identified when we examined within-participant variability – i.e. fluctuations in HR within a particular individual, within a testing session. Our analyses focused on the N250 component for Standard trials, and the P150/P3a component for Deviant trials, where significant group differences had been observed when examining between-participant differences in Analysis 1.

To examine this we compared the HR data recorded during each section with the concurrently recorded ERP responses (see Figure S10a). For each ERP response we calculated the average HR during the 15 seconds before and after the start of the trial. This relatively large time window was selected in order to preclude the possibility that regular vagally mediated changes may have influenced the per-trial HR scores. Individual trials were rank ordered according to the participant's HR at the time of the trial. Participant by participant, trials were then subdivided using a median split into 'high HR' and 'low HR' trials. Note that, because this split was performed separately for each participant, this analysis examines within-participant variability independent of between-participant variability in mean HR. Thus, the relationships shown here are entirely independent of the relationships shown in Analysis 1.

The results are shown in Figures S10b and S10c. For these plots, the individual datapoints show the average ERP amplitudes recorded for high HR (x-axis) and low HR (y-axis) trials. Figure S10b shows the Standard N250 amplitudes; a position above the 1:1 equivalence line indicates that, for that participant, the high HR trials showed higher amplitude (less negative) responses. Figure S10c shows the Deviant P150/P3a amplitudes; a position above the 1:1 line indicates that, for that participant, the high HR trials showed higher amplitude (more positive) responses. Paired-sample t-tests were conducted to compare amplitudes observed on high and low HR trials. Because both effects observed were directionally consistent with our predictions based on Analysis 1, one-tailed hypotheses were used. Significantly lower-amplitude N250 responses to Standard were observed during the high HR trials $t(20)=1.8$, $p=.047$. Results for the P150/P3a Deviant analysis (Figure 7c) include a clear outlier, more than 2 IQR from the mean. After this outlier was removed the results suggested that, although the effect observed was directionally consistent with our predictions, the result was not significant $t(19)=.99$ $p=.17$. The reason for this non-significant result is likely due to the lower sample size for this analysis (60 deviant trials per participant vs 280 standard trials).

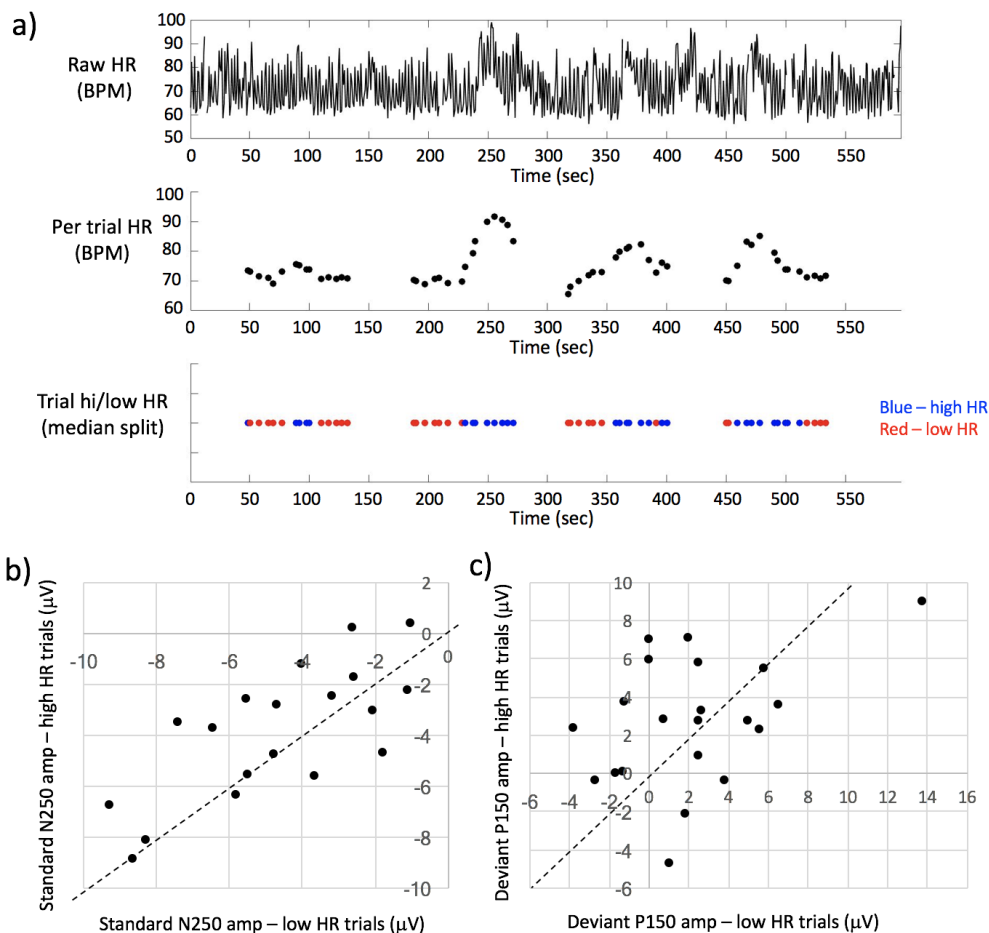


Figure S10: a) Illustrative sample from a single participant. Top: the raw, continuous HR data recorded during the session; Middle, the per trial HR, calculated as the average HR in the 15 seconds before and after the start of the trial; Bottom, the trials subdivided, participant by participant, by mean HR at the time of the trial. b) Average N250 amplitude for Standard trials, subdivided by mean HR at the time of the trial; x-axis shows the amplitude for high HR trials and y-axis shows the amplitude for low HR trials. The dashed line shows the 1:1 equivalence line: a position above this line indicates that, for that participant, the average amplitude for high HR trials was lower than that for low HR trials. c) Average P150 amplitude for Deviant

trials, subdivided by mean HR at the time of the trial. X-axis shows the amplitude for high HR trials and y-axis shows the amplitude for low HR trials. The dashed line shows the 1:1 equivalence line: a position above this line indicates that, for that participant, the average amplitude for high HR trials was higher than for low HR trials.

Supplementary References

- Berntson, G. G., Thomas Bigger, J., Eckberg, D. L., Grossman, P., Kaufmann, P. G., Malik, M., . . . Stone, P. H. (1997). Heart rate variability: origins, methods, and interpretive caveats. *Psychophysiology*, *34*(6), 623-648.
- Billman, G. E. (2013). The LF/HF ratio does not accurately measure cardiac sympatho-vagal balance. *Frontiers in physiology*, *4*.
- Bush, N. R., Alkon, A., Obradović, J., Stamperdahl, J., & Boyce, W. T. (2011). Differentiating challenge reactivity from psychomotor activity in studies of children's psychophysiology: Considerations for theory and measurement. *Journal of Experimental Child Psychology*, *110*(1), 62-79.
- Cacioppo, J. T., Tassinary, L. G., & Berntson, G. G. (2000). *Handbook of Psychophysiology* (2nd ed.): Cambridge University Press, Cambridge, UK.
- Johnson, N. L., Kotz, S., & Balakrishnan, N. (1994). Continuous Univariate Probability Distributions,(Vol. 1): John Wiley & Sons Inc., NY.
- Kushnerenko, E., Ceponiene, R., Balan, P., Fellman, V., & Näätänen, R. (2002). Maturation of the auditory change detection response in infants: a longitudinal ERP study. *NeuroReport*, *13*(15), 1843-1848.
- Lacouture, Y., & Cousineau, D. (2008). How to use MATLAB to fit the ex-Gaussian and other probability functions to a distribution of response times. *Tutorials in Quantitative Methods for Psychology*, *4*(1), 35-45.
- Porges, S. W. (1995). Cardiac vagal tone: a physiological index of stress. *Neurosci Biobehav Rev*, *19*(2), 225-233.
- Porges, S. W. (2007). The polyvagal perspective. *Biological Psychology*, *74*(2), 116-143. doi:10.1016/j.biopsycho.2006.06.009
- Reyes del Paso, G. A., Langewitz, W., Mulder, L. J., Roon, A., & Duschek, S. (2013). The utility of low frequency heart rate variability as an index of sympathetic cardiac tone: a review with emphasis on a reanalysis of previous studies. *Psychophysiology*, *50*(5), 477-487.